

Shape Similarity by Fractal Dimensionality: An Application in the *de novo* Design of (–)-Englerin A Mimetics

Lukas Friedrich^{+, [a]}, Ryan Byrne^{+, [a]}, Aaron Treder,^[b] Inderjeet Singh,^[b] Christoph Bauer,^[a] Thomas Gudermann,^[b, c, d] Michael Mederos y Schnitzler,^[b, c] Ursula Storch,^[b, e] and Gisbert Schneider^{*[a]}

Molecular shape and pharmacological function are interconnected. To capture shape, the fractal dimensionality concept was employed, providing a natural similarity measure for the virtual screening of *de novo* generated small molecules mimicking the structurally complex natural product (–)-englerin A. Two of the top-ranking designs were synthesized and tested for their ability to modulate transient receptor potential (TRP) cation channels which are cellular targets of (–)-englerin A. Intracellular calcium assays and electrophysiological whole-cell measurements of TRPC4 and TRPM8 channels revealed potent inhibitory effects of one of the computer-generated compounds. Four derivatives of this identified hit compound had comparable effects on TRPC4 and TRPM8. The results of this study corroborate the use of fractal dimensionality as an innovative shape-based molecular representation for molecular scaffold-hopping.

Virtual library compound screening is one of the major techniques employed in the identification of bioactive mole-

cules in drug discovery. The common underlying principle of the various computational approaches, ranging from compound database searching to automated *de novo* design, is the definition, quantification, and utilization of molecular similarity. Any similarity approach must encapsulate some features correlated with aspects of interest to the chemist, and, ideally, extend that correlation to provide useful perspectives on chemical space. Various methods have been proposed and utilized successfully to rank virtual and real compound libraries predicated on physicochemical properties, topological indices, and higher-dimensional methods incorporating information on the distribution of such properties in Euclidean (or other) spaces. Each of these are to a greater-or-lesser extent correlated with the implicit similarity measure most often of interest for drug design; that molecules grouped by some measure should have recognizably related biological activities.^[1–4]

The shape of a molecule has been observed to correlate with that of its binding pocket.^[5–8] One commonly-employed means of capturing this shape information is through alignment-based methods. Prominent approaches in this group utilize the maximum possible overlap in the volume of pairs of molecules to compare and rank query molecules against a template compound.^[9,10] Alignment-independent methods have been gaining in popularity, primarily owing to their speed.^[11,12] These provide a straightforward description of the distance distribution between heavy atoms in a molecule and a set of fixed reference points, but fail to consider molecular surface curvature. We here aim to introduce and provide a proof-of-concept of a novel means to rapidly describe and compare shape representations of molecular objects, enabling quick filtering of large compound libraries. To this end, we expand on the concepts elucidated in our earlier work in applying the concept of fractal dimensionality in fast, shape-based similarity-based virtual compound screening, and with minimal sampling of ligand conformational space.^[9] This approach allows for the description of a molecule through shape analysis of its Connolly surface,^[10] and for comparison of molecules through a simple distance measure.

To determine the utility of this shape-only method in molecular *de novo* design, we applied the fractal dimensionality descriptor to identify computationally generated, small molecule mimetics with similar biological activities to the structurally intricate ('complex') natural product (–)-englerin A (Figure 1). The sesquiterpene (–)-englerin A acts as a nanomolar activator of transient receptor potential canonical 4 and 5 (TRPC4/5) calcium-permeable cation channels which leads to selective

[a] Dr. L. Friedrich,⁺ R. Byrne,⁺ Dr. C. Bauer, Prof. Dr. G. Schneider
Department of Chemistry and Applied Biosciences
Swiss Federal Institute of Technology (ETH)
Vladimir-Prelog-Weg 4
8093 Zurich (Switzerland)
E-mail: gisbert.schneider@pharma.ethz.ch

[b] A. Treder, I. Singh, Prof. Dr. T. Gudermann, Prof. Dr. M. Mederos y Schnitzler,
Dr. U. Storch
Walther Straub Institute of Pharmacology and Toxicology
Ludwig Maximilians University of Munich
Goethestrasse 33
80336 Munich (Germany)

[c] Prof. Dr. T. Gudermann, Prof. Dr. M. Mederos y Schnitzler
DZHK (German Centre for Cardiovascular Research)
Munich Heart Alliance
Biedersteiner Strasse 29
80802 Munich (Germany)

[d] Prof. Dr. T. Gudermann
Comprehensive Pneumology Center Munich (CPC–M)
German Center for Lung Research
Max-Lebsche-Platz 31
81377 Munich (Germany)

[e] Dr. U. Storch
Institute for Cardiovascular Prevention (IPEK)
Ludwig Maximilians University of Munich
Pettenkoferstrasse 8a & 9
80336 Munich (Germany)

[†] These authors contributed equally to this work.

 Supporting information for this article is available on the WWW under <https://doi.org/10.1002/cmdc.202000017>

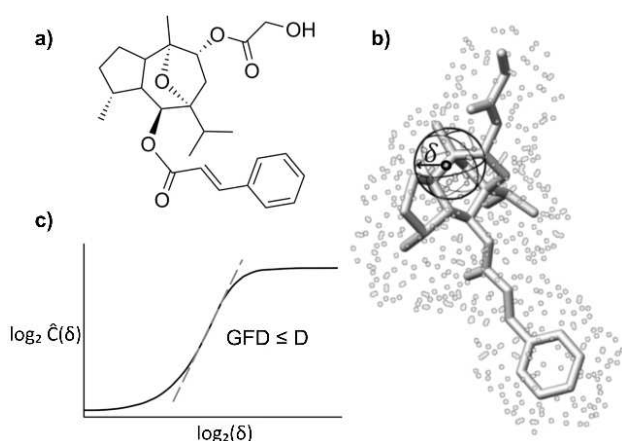


Figure 1. a) Molecular structure of the natural product (–)-englerin A, b) a discrete representation of its Connolly surface (grey dots) for a generated conformer, and c) an illustration of the behavior of the point-inclusion sphere, and the calculation of the fractal dimension, D . For each point in the surface representation, the relationship between the proportion of points ($\hat{C}(\delta)$) within a distance δ inclusion sphere and that distance is stored. These relationships are then combined, and described in terms of gradient, providing an unbiased estimation of the molecule's fractal dimensionality. GFD can be calculated for any small- or macro-molecule, and allows for shape-based screening based on a simple distance-from-template measure.

growth inhibition of cancer cell lines.^[11,12] Utilizing (–)-englerin A as a template, we previously generated small molecule mimetics by ligand-based, chemical reaction-driven *de novo* design.^[13] By topological pharmacophore-based scoring and manual refinement of the computational designs, we identified natural product mimetics inhibiting the TRP melastatin 8 (TRPM8) calcium permeable cation channel, also inhibited by (–)-englerin A.^[12,13] We here extend that preliminary original study by introducing the fractal dimensionality *pseudo*-metric. Given that the previously employed computational design method (*design of genuine structures*, DOGS)^[14] and the pharmacophore similarity metric (*chemically advanced template search*, CATS)^[15] each rely on two-dimensional molecular representations, we investigated the use of fractal dimensionality as an orthogonal similarity ranking approach, to take the spatial disposition of molecules into account. The library of 903 *in silico* structures employed in our previous study resulted in a set of 323 unique *de novo* designed small molecules, owing to redundancy in the original set of suggested molecules.

We ranked these computer-generated designs according to their Euclidean distance from (–)-englerin A in terms of their *global fractal dimensionality* (GFD) (Supplementary Information, Eq. (1)). To assess the potential of GFD as a shape-based descriptor for this target case, we conducted a comparative, retrospective, analysis of the chemical space retrieved by this method, against gold-standard structural fingerprint (*extended-connectivity fingerprints*, ECFP4),^[16] and two open-source methods, an alignment-free (*ultrafast shape recognition*, USR),^[17] and an alignment-based shape (*molecular overlay based on shape and electrostatic potential*, SHaEP)^[18] approach. Given that we lack a ground-truth in this case, *i.e.* experimental activity data for each molecule in our compound library, our retrospective

analysis adopts two approaches to assess the strengths and weaknesses of the proposed shape similarity method in identifying compounds of interest.

We begin with an analysis of three data sets; (i) the initial *de novo* design set (323 computer-generated molecules), (ii) the thirty top-ranked compounds in terms of global fractal dimensionality distance (GFD distance), and (iii) the thirty top-ranked compounds according to their topological pharmacophore similarity (CATS distance) to (–)-englerin A.^[15,19] Set (iii) was included to compare the GFD ranking approach with the CATS approach described previously.^[13] As a first approach, we extracted the molecular scaffolds ('Murcko scaffolds')^[20] of these compounds and analyzed their scaffold diversity in terms of the pairwise Jaccard-Tanimoto coefficient (T_c ; with values in the interval [0,1]) based on Morgan structural fingerprints (*radius* = 2; equivalent to ECFP4^[16]). The 323 initial *de novo* designs consisted of 152 unique scaffolds (47%) with high scaffold diversity (T_c = 0.18; lower values indicate greater diversity). The 30 top-ranked molecules according to GFD distance contained 24 unique (80%) and diverse (T_c = 0.17) scaffolds, whereas the 30 top-ranked compounds by CATS distance comprised 19 unique scaffolds (63%) with slightly lower diversity (T_c = 0.24). Only two scaffolds were present in both top-ranking sets (Supplementary Information).

Second, we employed an experimentally-validated target-prediction software developed in-house (*self-organizing map-based prediction of drug equivalence relationships*, SPiDER)^[21,22] to provide an estimate of the likelihood of a given compound being active against the target family 'Transient Receptor Potential Ion Channel'. The top 30 compounds retrieved by screening with the GFD, USR, SHaEP, and ECFP4 methods were analyzed to determine their predicted activity (number of compounds with an annotated $p < 0.05$) for the target family, and the proportion and diversity of the unique molecular scaffolds for the predicted active compounds. Out of 30 top-ranked designs, GFD retrieved nine compounds predicted as active, each with a unique scaffold and a high scaffold diversity (predicted actives = 9, proportion of unique scaffolds = 1.0, diversity of unique scaffolds (pairwise T_c) = 0.22). The SHaEP approach retrieved fewer predicted-active compounds, also all having unique scaffolds (6, 1.0, 0.21). USR retrieved the same number of predicted actives as the SHaEP approach, with fewer unique, but highly diverse, retrieved scaffolds (6, 0.66, 0.12). ECFP4 retrieved ten predicted actives, but with fewer, less diverse, unique scaffolds (10, 0.8, 0.33). Given that topological approaches were used in the processes of *de novo* library generation and target prediction, it is corroborative that the GFD approach, which treats sub-structural information implicitly, achieved a similar predicted-active retrieval performance under evaluation with topological methods. We also performed activity prediction and diversity analysis for the library in its entirety (predicted actives = 25%, scaffold diversity T_c = 0.18). In summary, SHaEP and USR had a slightly smaller proportion of predicted actives in their top-ranked lists (20% for each) than the entire set, with variation in number and diversity of retrieved scaffolds. ECFP4 and GFD retrieved ten and nine predicted actives (33% and 30% respectively), with GFD having

a higher, and highest-overall, number of unique molecular scaffolds in the predicted active compounds.

Calculated physicochemical properties of the GFD top-ranked compounds were comparable to both the initial *de novo* design set obtained with the DOGS software and the pharmacophore top-ranked compounds (CATS) (Supplementary Information).

For our prospective application, we applied the same selection rules as in the retrospective analysis yielding nine designs predicted as active out of the thirty top-ranked compounds according to their GFD distance to (–)-englerin A (Supplementary Information).

We selected compounds **1** and **2** for synthesis and bioactivity evaluation, considering their proposed synthetic routes by DOGS, their synthesizability^[23] and building block availability (Supplementary Information). For compound **1**, a piperidine extended derivative of the quinazolinone scaffold,^[24] no similar entries were found in ChEMBL24 by a substructure search.^[25] In a recent patent application,^[26] design **1** is present as a fragment in a series of phosphatidylinositol 3-kinase inhibitors. Of note, compound **2** contains a menthol moiety, a common substructure for TRP ion channel modulators, especially TRPM8,^[27] TRPA1,^[28] TRPV3, and TRPV4 (Supplementary Information). To the best of our knowledge, no meaningful pharmacological interaction between menthol-containing compounds and the TRPC4 ion channel has been shown to date.

The unmodified *in silico* structures **1** and **2** were synthesized following the proposed routes in three steps each (Figure 2). Condensation of (*rac*)-(2-piperidiny)methanamine (**3**) and isatoic anhydride (**4**) gave intermediate **5**. Cyclization of **5** with

formic acid followed by Boc-protection gave final product **1**. Compound **2** was synthesized from L-menthol (**6**) and (2*S*,3*aS*,6*aS*)-octahydrocyclopenta[*b*]pyrrole-2-carboxylic acid (**8**). Intermediate **7** was obtained by a Williamson ether formation of **6** and 2-chloroacetic acid. Esterification of **8** with benzyl alcohol gave intermediate **9**. Amide coupling of **7** and **9** using EDC/HOBt afforded compound **2**.

To assess their bioactivity profiles, we tested compound **1** and **2** in several TRP assays, in which (–)-englerin A showed activity (TRPC4, TRPM8, TRPA1, TRPV3, TRPV4).^[12] Since (–)-englerin A is a potent TRPC4 channel activator,^[11] we analyzed the modulatory effects of compound **1** and **2** on TRPC4 channels. Compound **1** had only a weak inhibitory effect of $\leq 20\%$ on TRPC4 currents at a concentration of 100 μM performing electrophysiological whole-cell measurements with TRPC4 over-expressing HEK293 cells (Supplementary Information). In contrast, compound **2** showed inhibitory effects on TRPC4 channels in the same electrophysiological assay (Figure 3a,b). (–)-Englerin A was used to elicit maximal TRPC4 currents. Application of stepwise increasing compound **2** concentrations in the presence of (–)-englerin A decreased the (–)-englerin A-induced TRPC4 currents (Supplementary Information). As a control, (–)-englerin A was applied for a second time inducing maximal TRPC4 currents which were used for normalization. The summary of the maximal outward currents induced by (–)-englerin A in the presence of compound **2** reveals an IC_{50} for compound **2** of $5.1 \pm 0.8 \mu\text{M}$ ($K_i = 0.9 \mu\text{M}$) (Figure 3b). Thus, we could identify compound **2** as a structurally novel TRPC4 channel blocker, and the first validation of an interaction of that channel with a menthol-containing com-

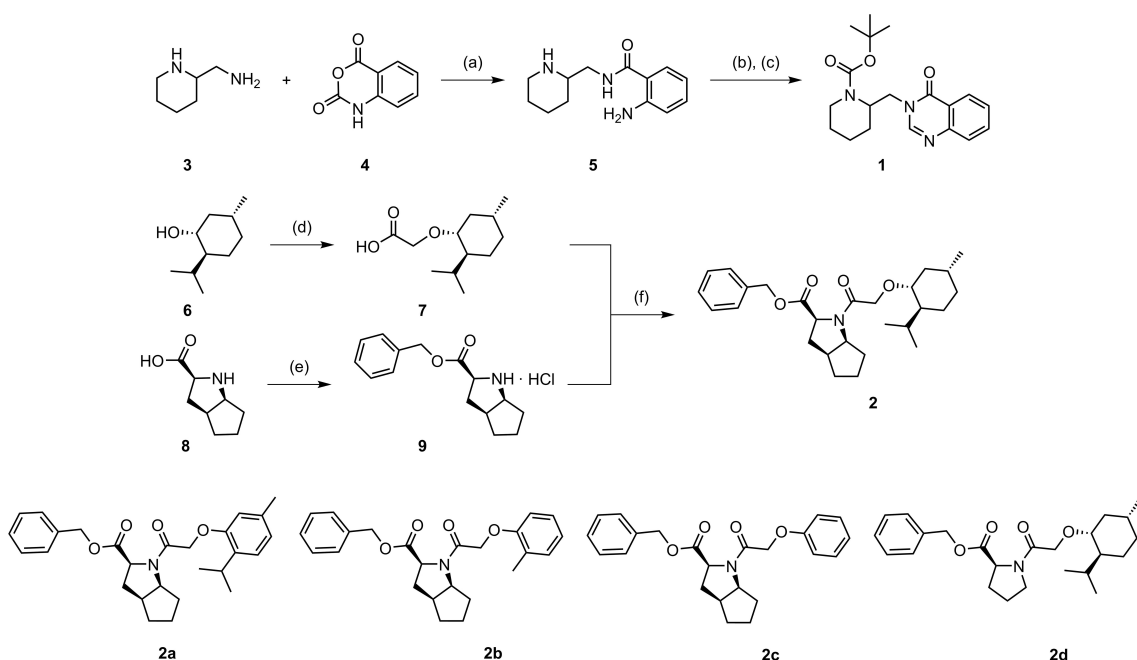


Figure 2. Synthesis of compound **1** and **2**. Reagents and conditions: (a) EtOH, reflux, 6 h, 37%; (b) formic acid, molecular sieves (4 Å), reflux, 6 h, 83%; (c) Boc_2O , NEt_3 , CH_2Cl_2 , 49%; (d) $\text{Cl}-\text{CH}_2-\text{COOH}$, NaH, KI, THF, 0 °C to reflux, 16 h, 18%; (e) HCl (in dioxane, 4 M), $\text{C}_6\text{H}_5-\text{CH}_2-\text{OH}$, SOCl_2 , 0 °C to rt, 70%; (f) EDC, HOBt, NEt_3 , THF, 0 °C to rt, 86%. Structural derivatives **2a–2d** of compound **2** were synthesized following the described synthetic route of compound **2** (Supporting Information).

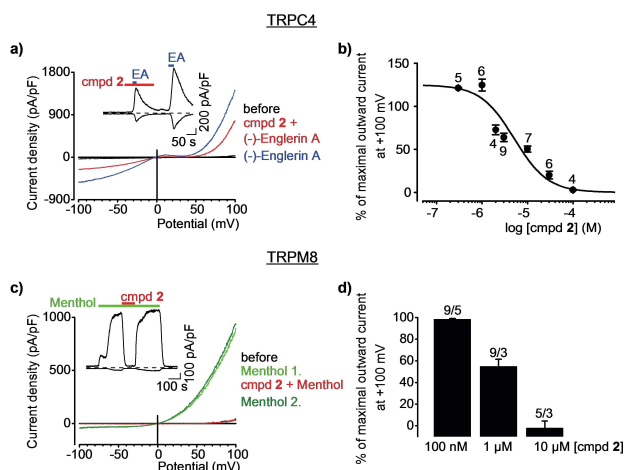


Figure 3. Electrophysiological whole-cell measurements of TRPC4 (a–b) or TRPM8 (c–d) overexpressing HEK293 cells. a) Representative current density-voltage curves before application of the first stimulus (black traces), during the first application of 50 nM (–)-englerin A ('EA') in the presence of indicated concentration (10 μM) of compound 2 ('cmpd 2 + EA', red traces) and during the second application of 50 nM (–)-englerin A (blue traces). b) Summary of maximal (–)-englerin A-induced outward currents in the presence of indicated concentrations of 2. Numbers indicate the number of measured cells from at least 3 independent experiments. To determine IC_{50} value the percentage of the maximal outward current at +100 mV elicited by the second application of 50 nM (–)-englerin A was used. Insets show current density time courses at holding potentials of ±100 mV with indicated applications of compound 2 (red), Menthol (green, a) and (–)-englerin A (blue, b). c) Representative current density-voltage curves before application of the first stimulus (black traces), during first application of 200 μM (–)-menthol ('Menthol 1', light green traces) and during application of indicated concentration (10 μM) of compound 2 in the presence of (–)-menthol ('cmpd 2 + Menthol', red traces). The dark green line indicates current density-voltage curve after washout of 2 in the presence of (–)-menthol ('Menthol 2', dark green traces). d) Summary of maximal (–)-menthol induced outward currents in the presence of indicated concentrations of compound 2. Numbers indicate the numbers of measured cells and the numbers of independent experiments. The percentage of the maximal outward current at +100 mV elicited by the first application of 200 μM (–)-menthol was used for normalization.

Compound 1 did not modulate ion channel TRPM8 at a concentration of 10 μM, whereas compound 2 showed an inhibitory effect in low micromolar concentration on TRPM8 ($IC_{50} = 1.8 \pm 1.1 \mu\text{M}$, $K_i = 0.3 \mu\text{M}$, Supplementary Information). The summary of the maximal (–)-menthol-induced outward currents in the presence of indicated compound 2 concentrations suggests that the half maximal inhibitory concentration of compound 2 is about 1 μM, which is in line with the results obtained with the intracellular calcium measurements. Compound 1 did not inhibit TRP ion channels TRPA1, TRPV3, and TRPV4 up to a concentration of 100 μM (Supplementary Information).

Compound 2 weakly inhibited TRPV4 ($IC_{50} = 39 \pm 1 \mu\text{M}$) and increased intracellular free calcium concentration in TRPA1 expressing cells during compound pre-incubation. Therefore, the measured inhibition of TRPA1 was likely caused by target desensitization (Supplementary Information).

To further validate the impact of molecular shape on bioactivity, and to obtain a preliminary local structure-activity relationship, four structural derivatives of compound 2 (2a–2d, Figure 2b) were synthesized, and their bioactivities on TRPC4 and TRPM8 assessed (Supplementary Information). All derivatives 2a–d exhibited weaker inhibition of TRPC4 channels than compound 2 (Supplementary Information), thereby rendering the GFD similarity metric non-quantitative with regard to biological activity. However, compounds 2a ($IC_{50} = 3.3 \pm 1.3 \mu\text{M}$, $K_i = 0.7 \mu\text{M}$), 2b ($IC_{50} = 2.5 \pm 1.1 \mu\text{M}$, $K_i = 0.6 \mu\text{M}$), and 2d ($IC_{50} = 2.7 \pm 1.1 \mu\text{M}$, $K_i = 0.6 \mu\text{M}$) blocked TRPM8 with similar efficiency as compound 2, with compound 2c ($IC_{50} = 10 \pm 1.1 \mu\text{M}$, $K_i = 2.2 \mu\text{M}$) yielding only slightly higher IC_{50} and K_i than compound 2 (Supplementary Information).

To exclude artefacts in activity measurement, we studied the aggregation behavior of compounds 2, 2a–d in water with dynamic light scattering. No aggregation of compound 2 was observed in concentrations <16 μM, and for 2a <62.5 μM. Compounds 2b–d, did not aggregate in concentrations <250 μM (2b) or <500 μM (2c, 2d), respectively (Supplementary Information).

Comparing the computational method employed here to existing shape-based screening approaches, our approach offers a molecular shape representation rooted in a well-established field of mathematics, which captures information about local surface curvature as well as volumetric information, and which can be rapidly calculated for large compound libraries. That said, an assessment of the merits and limitations of this approach on a broader basis is necessary before we can draw firm conclusions as to its general applicability. The experimental results of this proof-of-principle study reveal the potential of fractal dimensionality as a shape-based descriptor in ligand-based virtual screening and *de novo* molecular design. Given a limited sampling of ligand conformational space, we were able to identify a compound with potent inhibitory properties and a comparable activity profile to our template (–)-englerin A, based on the similarity in shape and local curvature of a library of small molecules generated through a *de novo* approach to our template (–)-englerin A. The combination of a novel shape-based approach, together with a *de novo* design tool and pharmacophore- and descriptor-driven target prediction software, proved useful in this instance. The extent to which this applies to other natural products, and to larger sets of small molecules, is a matter for further investigation.

Acknowledgements

We thank the Small Molecule Crystallography Center of ETH Zurich for X-ray services, Dr. Bernhard Pfeiffer for NMR services, and Sarah Haller for technical support. We also thank Thomas Voets for providing human TRPM8 channel in pCAGGSM2-IRES-GFP expression vector. This project has received funding from the European Union's Framework Programme for Research and Innovation Horizon 2020 (2014–2020) under the Marie Skłodowska-Curie Grant Agreement No. 675555 (AEGIS). This work was

supported by German Research Foundation (Deutsche Forschungsgemeinschaft projects no. 406028471 and TRR-152).

Keywords: natural products · virtual screening · drug discovery · molecular shape · computer-assisted drug design

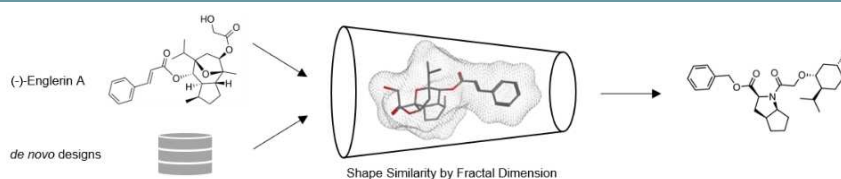
- [1] G. Maggiora, M. Vogt, D. Stumpfe, J. Bajorath, *J. Med. Chem.* **2014**, *57*, 3186–3204.
- [2] Y. Hu, D. Stumpfe, J. Bajorath, *J. Med. Chem.* **2016**, *59*, 4062–4076.
- [3] G. Schneider, *Drug Discovery Today Technol.* **2013**, *10*, e453–e460.
- [4] M. Weisel, E. Proschak, J. M. Kriegl, G. Schneider, *Proteomics* **2009**, *9*, 451–459.
- [5] S. Kortagere, M. D. Krasowski, S. Ekins, *Trends Pharmacol. Sci.* **2009**, *30*, 138–147.
- [6] A. Kahraman, R. J. Morris, R. A. Laskowski, J. M. Thornton, *J. Mol. Biol.* **2007**, *368*, 283–301.
- [7] K. Yeturu, N. Chandra, *BMC Bioinf.* **2008**, *9*, 543.
- [8] P. C. D. Hawkins, A. G. Skillman, A. Nicholls, *J. Med. Chem.* **2007**, *50*, 74–82.
- [9] N. Todoroff, J. Kunze, H. Schreuder, G. Hessler, K.-H. Baringhaus, G. Schneider, *Mol. Inf.* **2014**, *33*, 588–596.
- [10] M. L. Connolly, *J. Appl. Crystallogr.* **1983**, *16*, 548–558.
- [11] Y. Akbulut, H. J. Gaunt, K. Muraki, M. J. Ludlow, M. S. Amer, A. Bruns, N. S. Vasudev, L. Radtke, M. Willot, S. Hahn, T. Seitz, S. Ziegler, M. Christmann, D. J. Beech, H. Waldmann, *Angew. Chem. Int. Ed.* **2015**, *54*, 3787–3791; *Angew. Chem.* **2015**, *127*, 3858–3862.
- [12] C. Carson, P. Raman, J. Tullai, L. Xu, M. Henault, E. Thomas, S. Yeola, J. Lao, M. McPate, J. M. Verkuyl, G. Marsh, J. Sarber, A. Amaral, S. Bailey, D. Lubicka, H. Pham, N. Miranda, J. Ding, H.-M. Tang, H. Ju, P. Tranter, N. Ji, P. Krastel, R. K. Jain, A. M. Schumacher, J. J. Loureiro, E. George, G. Berellini, N. T. Ross, S. M. Bushell, G. Erdemli, J. M. Solomon, *PLoS One* **2015**, *10*, e0127498.
- [13] L. Friedrich, T. Rodrigues, C. S. Neuhaus, P. Schneider, G. Schneider, *Angew. Chem. Int. Ed.* **2016**, *55*, 6789–6792; *Angew. Chem.* **2016**, *128*, 6901–6904.
- [14] M. Hartenfeller, H. Zettl, M. Walter, M. Rupp, F. Reisen, E. Proschak, S. Weggen, H. Stark, G. Schneider, *PLoS Comput. Biol.* **2012**, *8*, e1002380.
- [15] M. Reutlinger, C. P. Koch, D. Reker, N. Todoroff, P. Schneider, T. Rodrigues, G. Schneider, *Mol. Inf.* **2013**, *32*, 133–138.
- [16] D. Rogers, M. Hahn, *J. Chem. Inf. Model.* **2010**, *50*, 742–754.
- [17] P. J. Ballester, W. G. Richards, *J. Comput. Chem.* **2007**, *28*, 1711–1723.
- [18] M. J. Vainio, J. S. Puranen, M. S. Johnson, *J. Chem. Inf. Model.* **2009**, *49*, 492–502.
- [19] G. Schneider, W. Neidhart, T. Giller, G. Schmid, *Angew. Chem. Int. Ed.* **1999**, *38*, 2894–2896; *Angew. Chem.* **1999**, *111*, 3068–3070.
- [20] G. W. Bemis, M. A. Murcko, *J. Med. Chem.* **1996**, *39*, 2887–2893.
- [21] D. Reker, T. Rodrigues, P. Schneider, G. Schneider, *Proc. Natl. Acad. Sci. USA* **2014**, *111*, 4067–4072.
- [22] D. Reker, A. M. Perna, T. Rodrigues, P. Schneider, M. Reutlinger, B. Mönch, A. Koeberle, C. Lamers, M. Gabler, H. Steinmetz, R. Müller, M. Schubert-Zsilavec, O. Werz, G. Schneider, *Nat. Chem.* **2014**, *6*, 1072–1078.
- [23] P. Ertl, A. Schuffenhauer, *J. Cheminf.* **2009**, *1*, 8.
- [24] E. Jafari, M. R. Khajouei, F. Hassanzadeh, G. H. Hakimelahi, G. A. Khodarahmi, *Res. Pharm. Sci.* **2016**, *11*, 1–14.
- [25] M. Davies, M. Nowotka, G. Papadatos, N. Dedman, A. Gaulton, F. Atkinson, L. Bellis, J. P. Overington, *Nucleic Acids Res.* **2015**, *43*, W612–W620.
- [26] S. Cai, Z. Du, J. Kaplan, J. A. Loyer-Drew, D. Naduthambi, B. W. Phillips, G. Phillips, J. Van Veldhuizen, W. J. Watkins, S. C. Yeung, **2015**, US2015/0361068A1.
- [27] M. J. Pérez De Vega, I. Gómez-Monterrey, A. Ferrer-Montiel, R. González-Muñiz, *J. Med. Chem.* **2016**, *59*, 10006–10029.
- [28] Y. Karashima, N. Damann, J. Prenen, K. Talavera, A. Segal, T. Voets, B. Nilius, *J. Neurosci.* **2007**, *27*, 9874–9884.

Manuscript received: January 10, 2020

Revised manuscript received: February 9, 2020

Version of record online: ■■■, ■■■■

COMMUNICATIONS



The shape of molecules can be described in terms of their fractal dimension, a measure of the 'complexity' of the molecular surface. A set of de novo designs was ranked according to fractal dimension similarity to the natural product template (-)-englerin A. One high ranked

compound potentially blocked TRPC4 and TRPM8 ion channels. The study shows the potential of fractal dimensionality as a molecular shape representation for virtual screening, scaffold-hopping, and ligand-based drug discovery.

Dr. L. Friedrich, R. Byrne, A. Treder, I. Singh, Dr. C. Bauer, Prof. Dr. T. Gudermann, Prof. Dr. M. Mederos y Schnitzler, Dr. U. Storch, Prof. Dr. G. Schneider*

1 – 6

Shape Similarity by Fractal Dimensionality: An Application in the de novo Design of (-)-Englerin A Mimetics

